Available online at www.sciencedirect.com
ScienceDirect
Acta Biomaterialia 2 (2006) 641–650
Acta BIOMATERIALIA
www.actamat-journals.com

# Controlled release of 5-fluorouridine from radiation-crosslinked poly(ethylene-co-vinyl acetate) films

Alvaro A.A. de Queiroz [a,*], Gustavo A. Abraham [b], Olga Zazuco Higa [c]

[a] *Departamento de Física e Química, Instituto de Ciências Exatas – Universidade Federal de Itajubá (UNIFEI), Av. BPS. 1303, 37500-903 Itajubá, Minas Gerais, Brazil*

[b] *Instituto de Investigaciones en Ciencia y Tecnología de Materiales, INTEMA (UNMdP-CONICET), J.B. Justo 4302, B78608FDQ, Mar del Plata, Argentina*

[c] *Instituto de Pesquisas Energéticas e Nucleares – IPEN/CNEN, SP, Brazil*

Received 14 December 2005; received in revised form 20 May 2006; accepted 23 May 2006

**Abstract**

The effect of γ-radiation doses of 12.5–380 kGy on the infrared spectra, gel content, mechanical properties, and the release of oxobutyl-5-fluoro-2′-deoxyuridine (OfdUrd, an antitumor agent) from poly(ethylene-co-vinyl acetate) (EVA) films was studied. The results showed that the application of radiation doses produced a crosslinking reaction leading to a maximum gel content of about 85% in the case of 150 kGy. Higher doses did not increase the gel content in EVA films. The mechanical properties (tensile strength, percentage elongation at break and Young's modulus) of all studied EVA matrices were affected by the exposure to γ-radiation. Irradiation doses over 50 kGy caused an increase in the Young's modulus of EVA and at the same time a decrease in the strain per cent. Moreover, the network structure formed after irradiation reduced significantly the OFdUrd release from EVA films. In this manner, the radiation dose applied to the polymeric matrix modulated the release of OFdUrd, avoiding the high concentrations that may cause severe systemic toxicity. The loading of OFdUrd to EVA film triggered a slight hyperemia after implantation, while the inflammatory reaction was only observed during the first two days.
© 2006 Acta Materialia Inc. Published by Elsevier Ltd. All rights reserved.

*Keywords:* Controlled release; Cancer treatment; 5-Fluorouridine; Crosslinked EVA; Radiation-crosslinking

## 1. Introduction

5-Fluorouracil (5-fluoro-2,4(1*H*,3*H*)-pyrimidinedione) (Scheme 1) is a potent antitumor agent that has been used in chemotherapy. 5-Fluorouracil (5-FU) is a pyrimidine antagonist widely used in the chemoradiotherapy treatment of cancer [1,2].

Several mechanisms of 5-FU action have been proposed, including inhibition of RNA function and/or processing and synthesis of thymidylate through inhibition of thymidylate synthetase, an enzyme which is inside the cancer cells, and thereby exerts its anticancer effect on the cells [3].

Despite the remarkable progress achieved in the reduction of incidence in developed countries, cervical cancer is still one of the major causes of cancer death worldwide. Previous studies have pointed out that 466,000 women are reported to develop cervical cancer around the world each year, and that 225,000 die from the disease. Approximately 80–85% of these deaths occur in women of developing countries in regions such as sub-Saharan Africa, South Asia and Latin America [4–8]. Unfortunately the exact cause of cervical cancer is unknown. But it is well known that the infection with two types of human papilloma virus, which is transmitted sexually, is strongly associated with cervical cancer and is the primary risk factor [9–12].

The administration of 5-fluorouracil in cervical cancer treatment is accompanied by severe toxic side effects and

* Corresponding author. Tel.: +55 35 3629 1435; fax: +55 35 3629 1140.
*E-mail address:* alencar@unifei.edu.br (A.A.A. de Queiroz).

1742-7061/$ - see front matter © 2006 Acta Materialia Inc. Published by Elsevier Ltd. All rights reserved.
doi:10.1016/j.actbio.2006.05.010

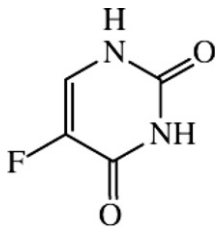

Scheme 1. 5-Fluorouracil.

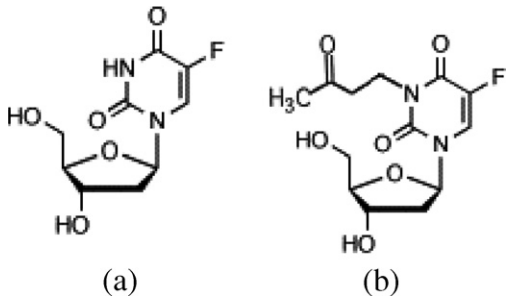

Scheme 2. Structures of 5-FdUrd and their derivative OFdUrd.

delivery problems [13–15]. More recently, drug delivery systems containing a prodrug of 5-FU, (+)-5-fluoro-2′-deoxyuridine (5-FdUrd) and derivatives (Scheme 2a), have been reported to be more effective in terms of avoiding some of the collateral effects of 5-FU administration [16–18]. Fluorouridine is a deoxyribonucleoside derivative of 5-FU that has been found to be a highly effective compound for the treatment of various solid tumors [19–21].

Chemotherapy using 5-FdUrd prodrugs in conjunction with radiotherapy has been shown to improve the outcome in cancer treatment. Radiotherapy generates radicals in cellular DNA and adjacent molecules that lead to the cancer cell death. Oxygen is important because it intercepts the short-lived free radicals and enhances DNA damage. Tumor cells lacking oxygen are radiotherapy resistant, but drugs that are more toxic to such hypoxic cells can exploit this deficiency. In the radiotherapy/chemotherapy treatment the 5-FdUrd prodrugs produce drug free radicals to activate them. Oxygen has a higher electron affinity than the drug, and rapidly removes the extra electron off the drug radical. Thus oxygen in normal tissue protects against drug activation, and selectivity against the tumor is achieved.

In order to obtain good radiochemical yield in a minimal reaction time, some clinical studies have suggested that the addition of 2-oxoalkyl side chain to 5-FdUrd at the N(3) position (Scheme 2b) generates 5-FdUrd derivatives that are more effective in the cancer treatment due to the higher radiochemical yield (*G*-value) of these prodrugs [22,23]. In this sense, the oxoalkylated 5-FdUrd may be more potent than 5-FdUrd when used clinically in radiotherapy treatment.

During the past century, advances in polymer chemistry have resulted in the development of biocompatible polymer delivery devices that reliably release pharmaceutical compounds in a controlled and continuous fashion [24–26].

Most companies now provide polymer devices for controlled drug delivery based on poly(ethylene-co-vinylacetate) (EVA). EVA copolymer is composed of long chains of ethylene and vinyl acetate groups randomly distributed throughout the chains. EVA is an inexpensive polymer with biocompatible properties approved for human use by Food and Drug Administration [27–30]. The usefulness of EVA copolymer as a drug delivery system for several drugs of clinical interest has been well explored in the literature [31–33].

It is well known that it is necessary to sterilize all biomaterials after their fabrication and prior to their surgical placement to reduce the risk of infections and associated complications. The most commonly used sterilization techniques utilize heat, steam, radiation or a combination of these methods [34]. The selection of the correct sterilization technique for EVA implants is crucial to their physical and mechanical properties, and hence to their performance in medicine. Hospital steam sterilization techniques commonly use high moisture and temperatures in excess of 100 °C. Such temperatures can approach or exceed the thermal transition temperatures of EVA and potentially alter their physical and mechanical properties. Chemical sterilization by ethylene oxide is often used for polymers that are sensitive to heat and moisture. This is particularly true for EVA copolymers that are thermoplastic in nature and degrade by hydrolysis. However, chemical sterilization can potentially leave residues in harmful quantities on the surface and within the polymer. Recent studies regarding the toxicity of ethylene oxide sterilization have raised serious questions due to the carcinogenic properties of the residues left in the polymer [35,36]. These residues may be present in harmful quantities on the surface and within the polymer. In this sense, it is crucial that polymeric implants are subjected to adequate degassing or aeration subsequent to ethylene oxide sterilization so that the concentration of residual ethylene oxide is reduced to acceptable levels.

An effective method developed for the sterilization of materials used in biomedicine is sterilization using ionizing radiation (γ-rays and electron beams) [37]. The biggest advantage of radiation sterilization over other ethylene oxide methodology is that the medical device can be sterilized after packing, thus avoiding problems of recontamination [38].

Recently, our interest has been focused on the design of controlled drug delivery systems based on alkylated fluorouridine derivatives. In this study, we have investigated the release characteristics of the prodrug oxobutyl-FdUrd (OFdUrd) from the EVA matrix crosslinked by γ-irradiation. In spite of a few studies on the use of EVA as a carrier for controlled release of 5-FU [39], as far as the authors are aware, no investigations of the design of OFdUrd delivery systems based on radiation-crosslinked EVA devices have been reported yet. A combination of radiation-crosslinked EVA and OFdUrd, maintaining therapeutic levels for several days, may be helpful in the treatment of cervical cancer.

## 2. Experimental

### 2.1. Materials

The EVA random copolymer with vinyl acetate content of 28% was supplied by Politeno, Brazil. The crystallinity of the EVA, determined by differential scanning calorimetry, was about 20% and it had a melting temperature of 78 °C. The number average molecular weight ($M_n$) and weight average molecular weight ($M_w$) of EVA were 15,600 g mol$^{-1}$ and 53,000 g mol$^{-1}$, respectively. The polydispersity ($M_w/M_n$) of EVA was 3.5. The drug 5-fluorouridine (5-FdUrd) was obtained from Sigma and was used without further purification.

### 2.2. Prodrug synthesis

The prodrug *N*-(3-oxobutyl)-5-fluorouridine (OfdUrd) was prepared by reacting 5-fluorouridine with the appropriate chloroformate prepared from the corresponding alcohol [40]. The solid obtained was purified by recrystallization from ethylacetate/light petroleum. Elemental analysis and $^1$H NMR spectroscopy was in agreement with the expected structures.

### 2.3. Matrix preparation

A weighed amount of the dry OFdUrd powder (30 mg) was dispersed in 25 mL of dimethyl sulfoxide (DMSO) in a glass vial. The EVA copolymer (2.5 g) was dissolved in the drug suspension at 50 °C. This mixture was poured onto a siliconed glass plate and the solvent was allowed to evaporate off at room temperature (25 °C) overnight. The membrane was removed from the plate and dried for 48 h at room temperature under vacuum. The polymer matrix containing the drug was placed in a steel mold and melt-pressed at 100 °C under 5 MPa in an electrically heated press for 2 min to obtain films of uniform thickness (600 μm). The molding was cooled under compression to maintain the overall dimensional stability of films. Then, rectangular matrices were cut from the membrane and weighed accurately. The drug content was calculated from the weight ratio of drug and copolymer used. The drug content (OFdUrd) in EVA matrix was analyzed by using an ultraviolet–visible (UV–vis) spectrometer at 266 nm (Varian Cary spectrophotometer). A calibration curve of OFdUrd in DMSO was used as a reference.

### 2.4. Gamma irradiation

The $^{60}$Co-γ-irradiation source was performed using a 22,000 Ci activity $^{60}$Co source (Nuclear and Energetic Research Institute, IPEN/CNEN-SP). The EVA samples were γ-irradiated at 25 °C at a dose rate of 12.15 kGy s$^{-1}$ in polyethylene bags under a nitrogen atmosphere. The doses of gamma radiation ranging from 12.5 to 380 kGy were measured using a Perspex dosimeter red type 4034 BM (Harwell® Laboratory, UK).

### 2.5. Determination of gel fraction

In order to investigate the influence of gamma irradiation on the gelation of EVA, samples were immersed in *o*-xylene at 80 °C for 72 h, then refluxed in a Soxhlet extractor for 24 h. The remaining insoluble sample was rinsed with methanol and dried in a vacuum oven at 70 °C to a constant weight. The equilibrium swelling time was determined from the experiments and the gel fraction was calculated gravimetrically from the weight of the sample before and after swelling as follows:

$$\text{Gel } (\%) = \frac{m}{m_0} \cdot 100 \quad (1)$$

where $m_0$ is the initial weight of the film and $m$ is the weight of the insoluble part of the film. The results of the gel fraction reported in this work represent the average of three samples.

### 2.6. Stress–strain measurements

Uniaxial stress–strain experiments were conducted at room temperature on an Instron 4301 Universal Testing Machine. The tensile tests were carried out according to ASTM D638 standard recommendations, using a cross-head displacement rate of 50 mm/min. Self-tightening grips were used in tensile tests. The grips self-tighten as tension increases and no appreciable displacement was observed in the assayed samples. A minimum of five specimens from each batch were mechanically tested.

### 2.7. Infrared spectroscopy

Attenuated total internal reflectance–Fourier transform infrared (ATR–FTIR) spectra of thin films were performed using a Perkin Elmer Spectrum One infrared spectrometer equipped with an ATR accessory. The FTIR spectra were measured with a 45° multiple reflection ZnSe crystal. Each spectrum was based on 16 scans.

### 2.8. In vitro drug release studies

The release behavior of EVA films loaded with OFdUrd was studied in phosphate-buffered saline pH 7.4 at 37 °C. The loaded polymer was placed into thermostatized cells and phosphate buffer pH 7.4 was circulated through the cells at the rate of 10 mL h$^{-1}$, and collected every hour using an automatic fraction collector. The total volume of the solution in the vessel was 100 mL and the stirring rate was always constant. At intervals, 50 μL samples were drawn from the solution in order to follow the change in the concentration of OFdUrd. A maximum of 40 aliquots were taken so the vessel volume was considered constant. Drug release was maintained under sink conditions, which

means that the amount of OFdUrd released should not exceed 10% of its solubility in the medium. The concentration of the drug was determined by UV–vis spectroscopy (Cary 50) using a 1 cm path length microcuvette (50 μL volume) at 266 nm. Standards of 0.1–50 μg $mL^{-1}$ in saline solution were used to obtain a calibration curve.

### 2.9. In vivo evaluation

The Ethical Committee of the Institutional Animal Care and Use Committee (IAUC) of IPEN-CNEN/USP approved the animal experimentation. Anesthesia was induced using intraperitoneal injection of a mixture containing xylazine hydrochloride, 10 mg/kg (Rompum, Bayer) and ketamine hydrochloride, 75 mg/kg (Ketanest 50, Parke-Davis). Before implantation, films were sterilized by γ-radiation (25 kGy). The biocompatibility of drug-loaded films was investigated subcutaneously and in the cage-implant system, according to the procedure described in the literature [41,42]. Loaded dishes of 5.0 mm in diameter were implanted subcutaneously in the back of Wistar rats between 7 and 9 weeks old, weighing 200–250 g at the level of panniculus carnosa, and the exudates surrounding the implanted material within the cage system were collected for the quantification of the inflammatory components. Samples were taken and histopathological observations were made at 3, 7, 14 and 21 days after implantation. Medical grade silicone was used as control.

## 3. Results and discussion

### 3.1. Radiation-crosslinking and polymer characterization

Gelation in polymers is generally referred to as crosslinking of macromolecules by means of covalent bonds. Crosslinking most likely occurs due to combinations of the macromolecular EVA radicals created during $^{60}Co$ irradiation. One of the proposed mechanisms for the radiation crosslinking of EVA is presented in Scheme 3 [43].

Fig. 1a shows the relationship between the gel content and irradiation dose for EVA. Unirradiated samples were found to be soluble in hot xylene, but the solubility of irradiated samples was reduced significantly. It is shown in Fig. 1a that gel content of EVA increased rapidly up to dose of 50 kGy and doses greater than 100 kGy led to a slow increase of the gel content. This suggests that the increase in the irradiation dose up to 100 kGy leads to an increasing of the crosslinking density in EVA chains [44,45].

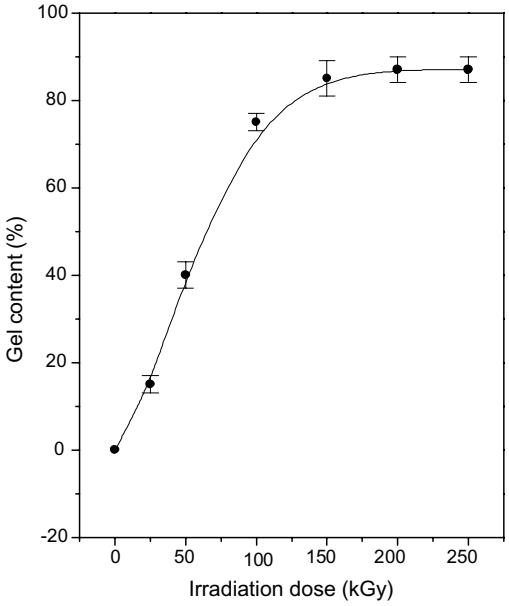


Fig. 1a. Variation of the gel content as a function of irradiation dose for EVA samples irradiated by gamma rays from $^{60}Co$ at room temperature (25 °C) and $N_2$ atmosphere.

According to the classical Charlesby–Pinner equation the relationships between the sol fraction $s$ and adsorbed dose ($D$) may be expressed by the equation [46]:

$$s + \sqrt{s} = \frac{p_0}{q_0} + \frac{2}{q_0 u_{2,0} D} \quad (2)$$

where $p_0$ and $q_0$ are constants which indicate sensitivity of dissociation and crosslinking to radiation, respectively.

The relationship between $s + s^{1/2}$ and $1/D$ shown in Fig. 1b is basically linear (regression coefficient, $r = 0.962$).

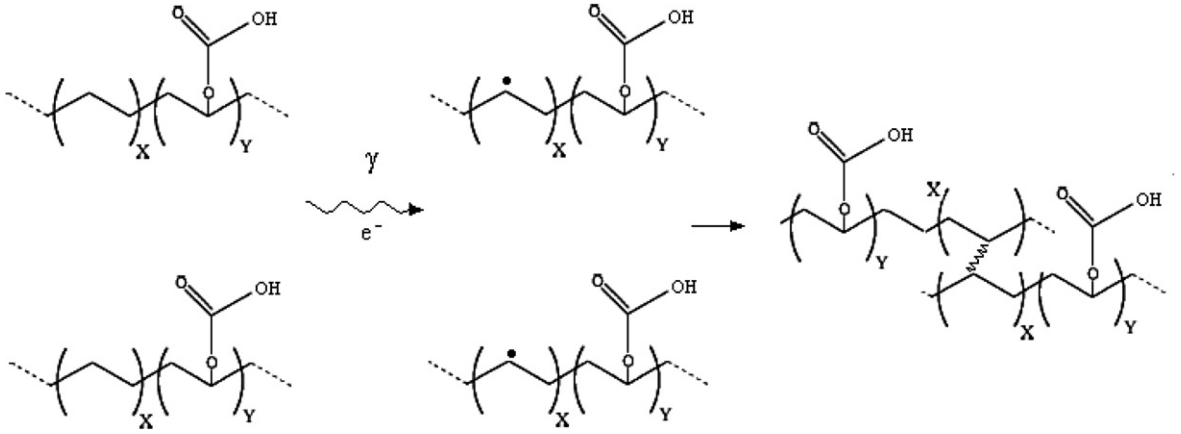


Scheme 3. Radiation crosslinking mechanism of EVA chains: radiation crosslinking by gamma rays (γ) or electron beam ($e^-$).

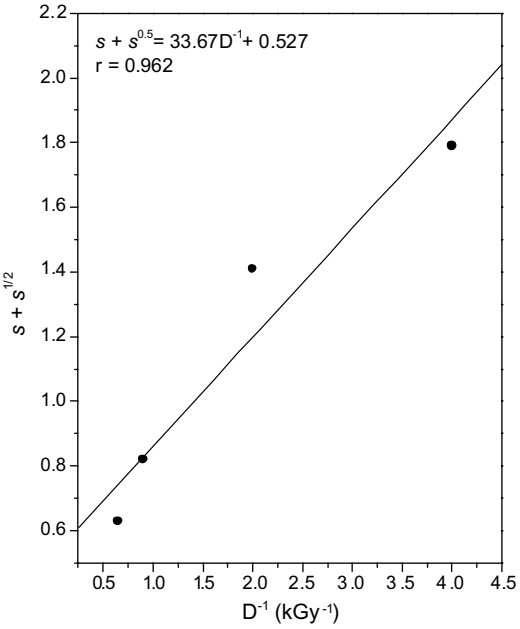


Fig. 1b. Sol–gel analysis plotted in the coordinates resulting from the classical Charlesby–Pinner equation. Dose rate: 12.15 kGy $s^{-1}$. Samples were irradiated in $N_2$ atmosphere.

This results suggests that radiation crosslinking of EVA matrix follows a random crosslinking law. However, the data points in Fig. 1b depart slightly from a straight line and this may be due to the fact that the molecular weight distributions in EVA may be not random prior to irradiation. From the plot of the dependence of $s + s^{1/2}$ on $1/D$, it is possible to obtain the gelation doses ($D_G$) and the ratio of probability of dissociation and crosslinking ($p_0/q_0$). In this work the $D_G$ and $p_0/q_0$ values for EVA matrix are 23 kGy and 0.53, respectively. The $p_0/q_0$ results suggests that EVA has a tendency to form crosslinks rather than scission, since $p_0/q_0 = 0.53$.

The Young's modulus of the γ-irradiated films as a function of the irradiation dose is shown in Fig. 2. It can be seen that Young's modulus also increased rapidly up to dose 50 kGy. A clear linear relationship was observed between irradiation dose and Young's modulus, indicating an increased stiffness of EVA matrix probably due to the formation of crosslinked EVA chains as confirmed by gel content results (Fig. 1).

Fig. 3 shows the stress–strain curves of EVA membranes as a function of irradiation dose. It was found that the strength of EVA increased gradually with increasing irradiation dose up to 114 kGy, while the strain per cent decreased with the radiation treatment. The behavior of EVA matrices after γ-irradiation is related to the formation of a crosslinked EVA structure as confirmed by gel content analysis. However, higher radiation doses produced a brittle film displaying a low strain per cent and may be a consequence of the high crosslinking density and the expected damage of the EVA structure [45].

The ATR–FTIR spectra of unirradiated and irradiated EVA films with 12.15 kGy $s^{-1}$ dose rates are shown in

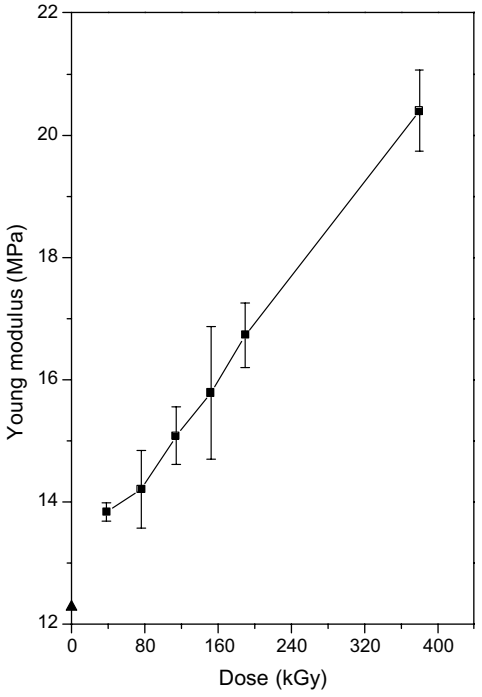


Fig. 2. Young's modulus behavior of EVA membranes (■) as a function of different radiation dose at 12.15 kGy $s^{-1}$ dose rate. Non-treated membrane is indicated with the symbol (▲).

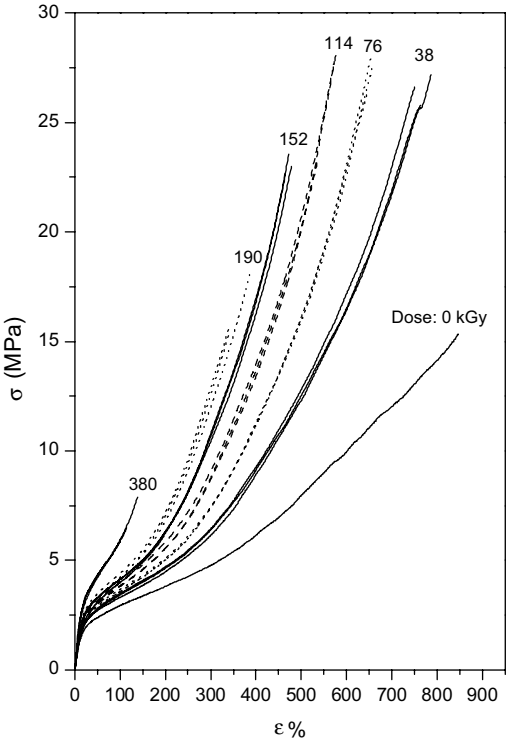


Fig. 3. Stress–strain curves of membranes with different radiation dose at dose rate of 12.15 kGy $s^{-1}$.

Fig. 4a and b. The spectra of pure EVA shows absorption peaks at 1740 $cm^{-1}$ due to carbonyl stretching (C=O) for ester carbonyl groups of vinyl acetate, 1470 $cm^{-1}$ due to

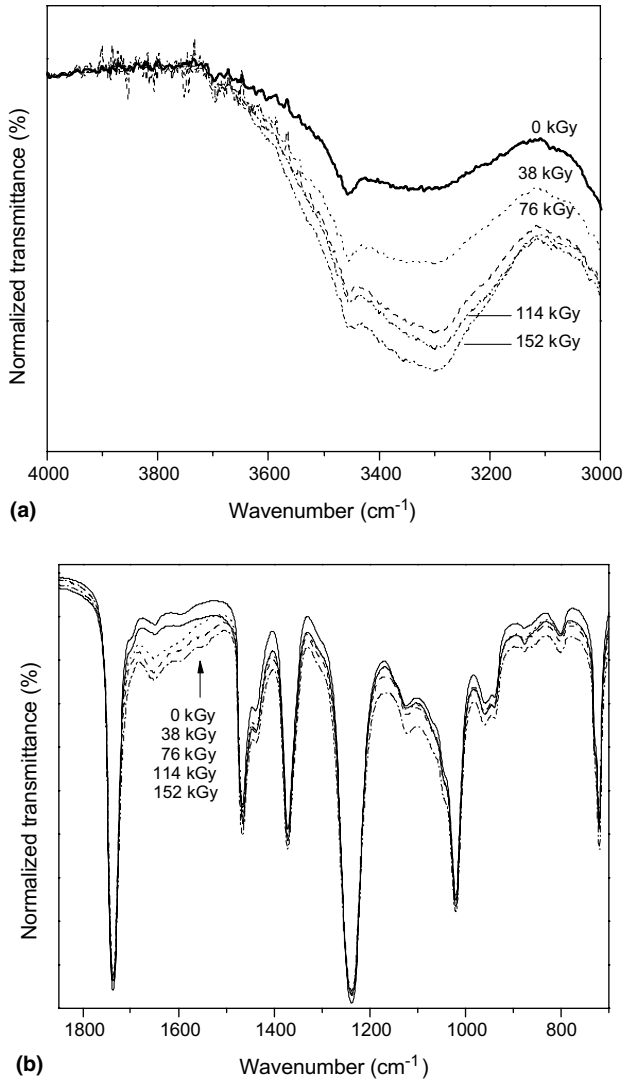


Fig. 4. ATR–FTIR spectra of EVA membranes at different dose (dose rate: 12.15 kGy $s^{-1}$). (a) Region 4000–3000 $cm^{-1}$ and (b) region 1850–700 $cm^{-1}$.

C–H bending of $CH_2$, 1370 $cm^{-1}$ due to C–H bending of $CH_3$, 1244 $cm^{-1}$ and 1030 $cm^{-1}$ due to C–O–C group. These peaks are in good agreement with the literature values [47].

The major species produced by the irradiation induced structural changes of EVA have been identified from their characteristic infrared absorption bands [48]. These species are: hydrogen-bonded hydroxyls (alcohols, hydroperoxides, carboxylic acids) at 3100–3600 $cm^{-1}$, carbonyls (ketones, acids, esters, etc.) at 1700–1800 $cm^{-1}$ and unsaturated carbon–carbon bonds (C=C) at 1600–1700 $cm^{-1}$. The increase of the broad band between 3000 and 3600 $cm^{-1}$ may be associated with an increase in the amount of hydroxyls. Furthermore, the peak at 3330 $cm^{-1}$ clearly identifies the increasing hydrogen-bonded hydroperoxides. The hydroperoxide band has a markedly higher intensity for the EVA samples having more than 100 kGy doses than for the original (unirradiated) sample. For comparison, the FTIR spectra of EVA samples having 0, 38, 78, 114 and 152 kGy doses are shown in Fig. 4a where the changes of the broad band between 3000 and 3600 $cm^{-1}$ may be clearly observed. For the carbonyl band (Fig. 4b), the unirradiated EVA sample have very weak (nearly at the level of detection limit) carbonyl and carboxyl peaks in the region at 1680 $cm^{-1}$, probably due to slight oxidation during the sample preparation. An increase in the dose to 100 kGy causes an increase in the absorbance peaks at 1680 $cm^{-1}$ (Fig. 4b).

It is well known that the higher irradiation doses may be able to promote other competitive reactions in EVA matrix and not only the crosslinked chains [44,45]. Our FTIR results suggest that at microscopic levels the changes in the ATR–FTIR spectra of irradiated EVA may be attributable to structural changes such as macromolecular chain splitting, creation of low mass fragments, production of free radicals, oxidation and crosslinking as result of the higher gamma radiation doses.

### 3.2. 5-Drug release

In order to study the effect of the EVA crosslinking on drug release kinetics, the release of OFdUrd dispersed in EVA matrices irradiated at different radiation doses was investigated. For a controlled diffusion process, the OFdUrd diffusion through EVA matrix can be expressed by the following equation [49]:

$$\frac{\partial c(x,t)}{\partial t} = D\frac{\partial^2 c(x,t)}{\partial x^2} \tag{3}$$

where $c$ represents the concentration of the drug at distance $x$ from the contacting surface and $D$ represents the diffusion coefficient.

The above equation has several solutions, depending on the boundary and, consequently, experimental conditions. The most commonly method used for determining the diffusion coefficient ($D$) is the gravimetric method or weight gain. The weight gain method consists of the study of the kinetics of liquid sorption by a polymer sample under isothermal and isobarical conditions. If the liquid-sorbing sample is a plate of thickness $L$, under the boundary conditions $0 < x < L$ and $0 < C < C_{\text{equilibrium}}$, Fick's second law after integration gives [50]:

$$\frac{M_t}{M_\infty} = \frac{4}{L}\left(\frac{D_{\text{OFdUrd}}.t}{\pi}\right)^{1/2} \quad \text{or} \quad x = 4\left(\frac{D_{\text{OFdUrd}}.t}{\pi}\right)^{1/2} \tag{4}$$

where $L(M_t/M_\infty)$ may be replaced by $x$, the position of the solution/polymer interface.

It is known that for polymers that are above their glass transition temperature ($T_g$) at the experimental conditions, as is the case for the EVA used in this work, the diffusion of the solvent is slower than the relaxation time of the polymer. In this case, the transport mechanism is denominated Fickian when the position of the penetrant front versus time is described by

$$x = kt^{1/2} \tag{5}$$

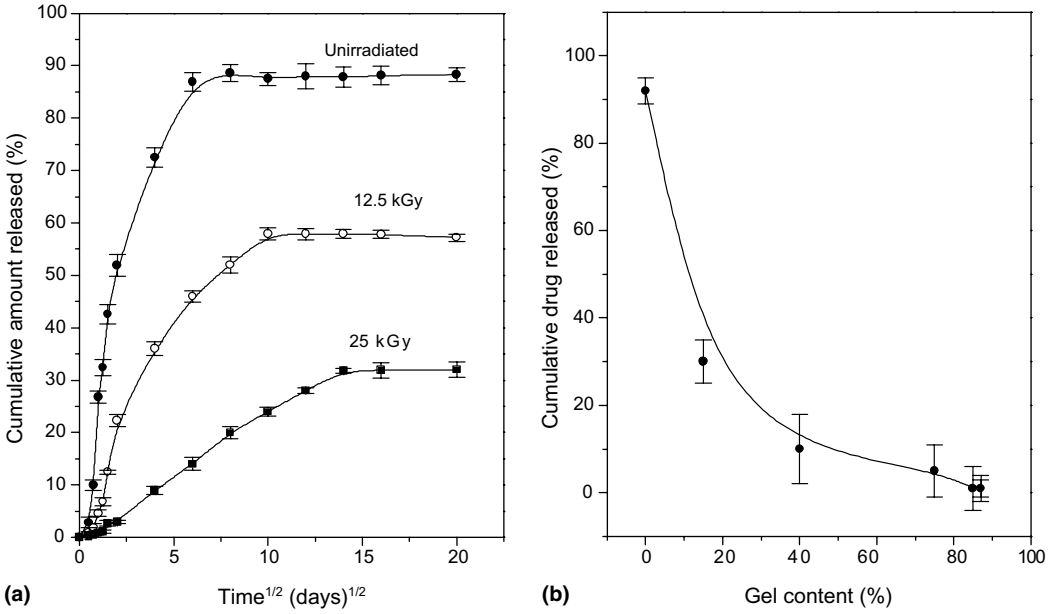


Fig. 5. Effect of radiation dose (a) and the gel content (b) on the cumulative release of OFdUrd from EVA matrices at 37 °C.

where $k$ is a proportional constant that is related to the square root of the diffusion coefficient, $D$.

Fig. 5a shows the OFdUrd release results, expressed as the cumulative amount of the drug OFdUrd released versus the square root of time ($t^{1/2}$). The variation of the drug released from the γ-irradiated and unirradiated EVA matrix was characterized by three phases (Fig. 5a): (i) an initial period of rapid release of OFdUrd (burst effect) due to the release of drug molecules at the matrix surface; (ii) a period where release of the OFdUrd drug was approximately linear with respect to $t^{1/2}$ and (iii) a final period when release tapered off, due to the increased difficulty of diffusion of drug occluded inside the matrix with decrease of the initial drug concentration in the membranes.

The OFdUrd release dependence of the gel content on the irradiation dose in γ-irradiated EVA matrix is given in Fig. 5b. As expected, the release rate decreased with increasing gel content. This can be explained by the decreased mobility of the EVA chains due to the increase in the crosslinking density. In this sense, the free volume available for the diffusion of drug molecules decreases, restraining the mobility and lowering the coefficient diffusion values of the OFdUrd drug through the EVA matrix.

Fig. 6 shows the apparent diffusion coefficient of OFdUrd drug through EVA films. The diffusion coefficient of OFdUrd decreased with the increase in the gel content indicating that the increase in the crosslinking density of the polymer matrix reduces the mobility of the aqueous medium in the EVA films. The reduction in the mobility of the EVA chain due to the radiation-crosslinking leads to the decrease in the diffusion coefficient values of OFdUrd. However, because the above data treatment method is quite simplified, it must be emphasized that the results of these calculations are only meant for comparative purposes within a given drug delivery system study, not to provide absolute values of diffusion coefficients.

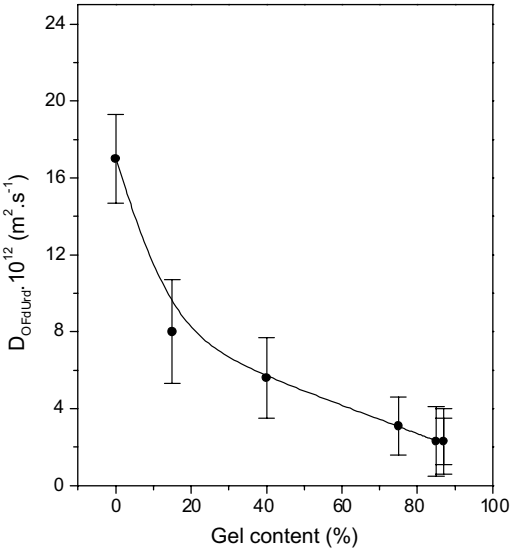


Fig. 6. Variation of the diffusion coefficient independent of the membrane loading for the OFdUrd release in PBS pH 7.4 from EVA matrix as a function of the gel content at 37 °C.

The morphology and appearance of the OFdUrd particles dispersed in EVA matrix were examined by scanning electron microscopy (SEM). Cross-sections of the EVA membranes were made using a microtome to study their inner structure. The SEM micrographs of the EVA and drug-loaded EVA matrices are shown in Fig. 7. The SEM micrograph of cross-sections of EVA matrix (Fig. 7a) revealed a smooth and compact structure without any noticeable pinholes or cracks within the conventional SEM resolution. Fig. 7b shows the presence of OFdUrd

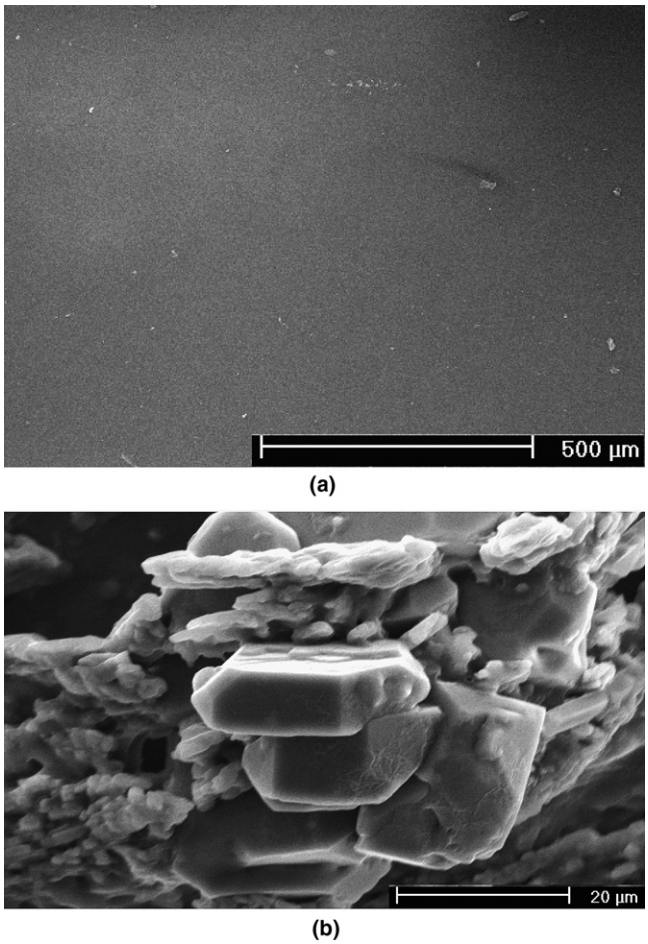


Fig. 7. SEM micrographs of a cross-section of EVA (a) and OFdUrd/EVA matrix (b).

crystals that may be associated with recrystallization of OFdUrd dissolved initially in the polymer matrix. Most probably the recrystallization of the drug occurs in the amorphous domains of the EVA and it may be severely hindered by the polymer matrix. In this case, it is expected that not all OFdUrd will crystallize in monodisperse form. As a consequence, the size of particles is polydisperse with a total range of 5–30 μm, as shown by SEM micrographs.

### 3.3. In vivo results

The implantation of synthetic materials in the human body is a procedure with a high risk of infection. It is well known that the potential for using of a polymer is strongly dependent on its biocompatibility. Accumulated experimental evidence suggests that a marked inflammatory reaction would counter the effect of the wound healing inhibitors. EVA biocompatibility has been extensively investigated and markedly improved by purifying the polymer of residual monomers and oligomers, and also by producing the polymer aseptically. In view of tissue response and biocompatibility, it is extremely important to consider the biological activity of the therapeutic agents incorporated into the carrier, especially if the bioactive agent has

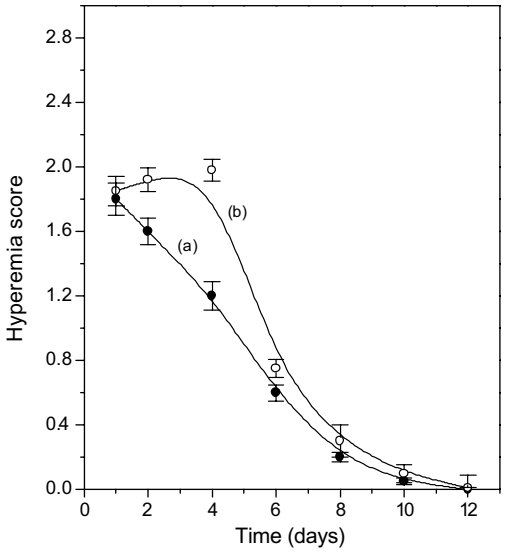


Fig. 8. Effect of OFdUrd/EVA matrix implantation on individual parameters of the tissue response in rats. (a) EVA and (b) OFdUrd/EVA.

cytotoxic or anti-inflammatory characteristics. The inherent toxicity of therapeutic agents must be considered as having the potential of altering the inflammatory (phase I) and foreign body reaction (phase II) [51,52]. In this sense, ISO standards 10993 regarding the biological evaluation of medical devices require various tests on the polymers or polymer carriers containing therapeutic agents.

Inflammation is the most potent effect of immune defense. It is recognized as swelling, pain, heat, and redness in the affected tissue. Immune cells within the biological tissue release specific mediators that control local circulation and cell activities, producing inflammation. Under the microscope, an inflamed tissue is seen to be invaded by a variety of immune cells. The rejection of implantable materials represents a chronic inflammatory process and inflammatory cell population markers like lymphocytes and release enzymes as alkaline phosphatases provide an adjunctive method for global assessment of biocompatibility.

Fig. 8 shows the hyperemia score after implantation of sterilized OFdUrd/EVA films. The concentrations of polymorphonuclear cells and lymphocytes as well as the extra- and intracellular activities of acid and alkaline phosphatases were not significantly different from the control. The loading of OFdUrd to EVA film triggered a slight hyperemia. However, the inflammatory reaction was only present during the first two days. No irreversible changes occurred in the tissues, indicating an overall good biocompatibility.

## 4. Conclusions

γ-Irradiation produced a crosslinked network in EVA films, as shown by the presence of a gel fraction, the content being increased with the irradiation dose. The change in the polymer structure had an important effect on the mechanical properties, as evidenced by the observed elastic

modulus and the ultimate strain values. The crosslinked network modulated the release of OFdUrd from the EVA films, avoiding the high concentrations that may cause severe systemic toxicity. Loaded EVA film showed a non-significant hyperemia, displaying a low inflammatory reaction after implantation. The results obtained in this work are promising for the design of drug delivery systems in which is necessary to control both the total amount of the drug released and the kinetic profile.

## Acknowledgements

G.A. Abraham thanks CONICET and ANPCyT (Argentina) for the partial financial support of this work. The authors would like to thank the CYTED network subprogram VIII. J ''Biomateriales para la salud''.

## References

[1] Truter EJ, Santos AS, ELS WJ. Assessment of the antitumour activity of targeted immunospecific albumin microspheres loaded with cisplatin and 5-fluorouracil: toxicity against a rodent ovarian carcinoma in vitro. Cell Biol Int 2001;25(1):51–9.
[2] Kurtz JE, Andrès E, Natarajan-Amé S, Noel E, Dufour P. Oral chemotherapy in colorectal treatment: review of the literature. Eur J Int Med 2003;14:18–25.
[3] Santi DV, McHenry CS, Sommer H. Mechanism of interaction of thymidylate synthetase with 5-fluorodeoxyuridylate. Biochemistry 1974;13:471–81.
[4] Critchlow CW, Kiviat NB. Old and new issues in cervical cancer control. J Natl Cancer Inst 1999;91(3):200–1.
[5] Monsonego J, Bosch FX, Coursaget P, Cos JT, Franco E, Frazer I. Cervical cancer control, priorities and new directions. Int J Cancer 2004;108:329–33.
[6] Seeff LC, McKenna MT. Cervical cancer mortality among foreign-born women living in the United States, 1985 to 1996. Cancer Detect Prev 2003;27:203–8.
[7] Parkin DM, Pisani P, Ferlay J. Estimates of the worldwide incidence of 25 major cancers in 1990. Int J Cancer 1999;80:827–41.
[8] Van Der Graaf Y, Zirlhius GA, Vooijs GP. Cervical cancer mortality in the Netherlands. Int J Epidemiol 1988;17:270–6.
[9] Bosch FX. Prevalence of human papillomavirus in cervical cancer: a worldwide perspective. J Natl Cancer Inst 1995;87(11):796–802.
[10] Kjaer SK, van den Brule AJC, Paull G, Svare EI, Sherman ME, Thomsen BL, et al. Type specific persistence of high-risk human papillomavirus (HPV) as indicator of high-grade cervical squamous intraepithelial lesions in young women: population based prospective follow up study. Br Med J 2002;325(7364):572–5.
[11] Rozendaal L, Walboomers JMM, van der Linden JC, Voorhorst FJ, Kenemans P, Helmerhorst TJ. PCR-based high-risk HPV test in cervical cancer screening gives objective risk assessment of women with cytomorphologically normal smears. Int J Cancer 1996;68:766–9.
[12] Woodman CBJ, Collin S, Winter H, Bailey A, Ellis J, Prior P, et al. Natural history of cervical human papillomavirus infection in young women: a longitudinal study. Lancet 2001;357:1831–6.
[13] Houghton JA, Houghton PJ, Wooten RS. Mechanism of induction of gastrointestinal toxicity in the mouse by 5-fluorouracil, 5-fluorouridine and 5-fluoro-2′-deoxyuridine. Cancer Res 1979;39:2406–13.
[14] Schuetz JD, Wallance HJ, Diasio RB. 5-Fluorouracil incorporation into DNA of CF-1 mouse bone marrow cells as a possible mechanism of toxicity. Cancer Res 1984;44:1358–63.
[15] Kimura Y, Okuda H. Prevention by carp extract of myelotoxicity and gastrointestinal toxicity induced by 5-fluorouracil without loss of antitumor activity in mice. J Ethnopharm 1999;68:39–45.
[16] Ulbrich K, Subr V. Polymeric anticancer drugs with pH-controlled activation. Adv Drug Deliv Rev 2004;56:1023–50.
[17] Huang DS. Uptake and clearance of 5-fluorouridine following subconjunctival and intravitreal injection. Retina 1988;8(3):205–9.
[18] Koning GA, Morselt HWM, Velinova MJ, et al. Selective transfer of a lipophilic prodrug of 5-fluorodeoxyuridine (FUdR) from immunoliposomes to colon cancer cells. Biochim Biophys Acta 1999;1420:153–67.
[19] van Laar JAM, Rustum YM, Ackland SP. Comparison of 5-fluoro-2′-deoxyuridine with 5-fluorouracil and their role in the treatment of colorectal cancer. Eur J Cancer 1998;34:296–306.
[20] Bartkowski R, Berger MR, Aguiar JL. Experiments on the efficacy and toxicity of locoregional chemotherapy of liver tumors with 5-fluoro-2′-deoxyuridine (FUDR) and 5-fluorouracil (FU) in an animal model. J Cancer Res Clin Oncol 1986;111:42–6.
[21] Shibamoto Y, Mimasu Y, Tachi Y. Comparison of 5-fluorouracil and 5-fluoro-2′-deoxyuridine as an effector in radiation-activated prodrug. J Chemother 2002;14:390–6.
[22] Shibamoto Y, Tachi Y, Tanabe K, Hatta H, Nishimoto SI. In vitro and in vivo evaluation of novel antitumor prodrugs of 5-fluoro-2′-deoxyuridine activated by hypoxic irradiation. Int J Radiat Oncol Biol Phys 2004;58(2):397–402.
[23] Steffansen B, Pearson PA, Buur A, Ashton P. Alkoxycarbonyl prodrugs of 5-ftuorouracil suspended in silicone oil as an intraocular sustained release system. Pharm Res 1992;9:S237.
[24] Baldwin SP, Saltzman WM. Materials for protein delivery in tissue engineering. Adv Drug Deliv Rev 1998;33:71–86.
[25] Lin DM, Kalachandra S, Valiyaparambil J, Offenbacher S. A polymeric device for delivery of anti-microbial and antifungal drugs in the oral environment: effect of temperature and medium on the rate of drug release. Dental Mater 2003;19:589–96.
[26] Langer R, Peppas AN. Advances in biomaterials, drug delivery and bionanotechnology. AIChE J 2003;49(12):2990–3006.
[27] Sam AP. Controlled release contraceptive devices: a status report. J Control Release 1992;22:35–46.
[28] Langer R, Brem H, Tapper D. Biocompatibility of polymeric delivery systems for macromolecules. J Biomed Mater Res 1981;15:167–277.
[29] Niemi SM, Fox JG, Brown LR, Langer R. Evaluation of ethylene–vinyl acetate copolymer as a non-inflammatory alternative to Freund's complete adjuvant in rabbits. Lab Anim Sci 1985;35:609–12.
[30] Shastri PV. Toxicology of polymers for implant contraceptives for women. Contraception 2002;65:9–13.
[31] Cho CW, Shin SC. Enhanced transdermal delivery of atenolol from the ethylene–vinyl acetate matrix. Int J Pharm 2004;287:67–71.
[32] Rafferty DW, Koenig JL. FTIR imaging for the characterization of controlled-release drug delivery applications. J Control Release 2002;83:29–39.
[33] Velayudhan S, Anilkumar TV, Kumary TV, Mohanan PV, Fernandez AC, Varma HK, et al. Acta Biomater 2005;1:201–9.
[34] Athanasiou KA, Niederauer GG, Agrawal M. Sterilization, toxicity, biocompatibility and clinical applications of polylactic acid/polyglycolic acid copolymers. Biomaterials 1996;17:93–102.
[35] Thier R, Bolt HM. Carcinogenicity and genotoxicity of ethylene oxide: new aspects and recent advances. Crit Rev Toxicol 2000;30(5):595–608.
[36] Holyoak GR, Wang S, Liu Y, Bunch TD. Toxic effects of ethylene oxide residues on bovine embryos in vitro. Toxicology 1996;108(1–2):33–8.
[37] Benson RS. Use of radiation in biomaterials science. Nucl Instrum Meth B 2002;191:752–7.
[38] Ishigaki I, Yoshii F. Radiation effects on polymer materials in radiation sterilization of medical supplies. Radiat Phys Chem 1992;39(6):527–33.
[39] Miyazaki S, Ishi K, Sugibayashi K, Morimoto Y, Takada M. Antitumor effect of ethylene–vinyl acetate copolymer matrices containing 5-fluorouracil on ehrlich ascites carcinoma in mice. Chem Pharm Bull 1982;30:3770–5.

[40] Buur A, Bundgaard H. Prodrugs of 5-fluorouracil V. l-Alkoxycarbonyl derivatives as potential prodrug forms for improved rectal or oral delivery of 5-fluorouracil. J Pharm Sci 1986;75:522–7.
[41] Marchant R, Hiltner A, Hamlin C, Rabinovitch A, Slobodkin R, Anderson JM. In vivo biocompatibility studies. The cage implant system and a biodegradable hydrogel. J Biomed Mater Res 1983;17:310–25.
[42] Yamaguchi K, Anderson JM. Biocompatibility studies of naltrexone sustained release formulations. J Control Release 1992;19:299–314.
[43] Dutta SK, Bhowmick AK, Chaki TK. Structure property relationship of ethylene vinyl acetate copolymer grafted with triallyl cyanurate by electron beam radiation. Radiat Phys Chem 1996;47(6):913–26.
[44] Mateev M, Karageorgiev S. The effect of electron beam irradiation and content of EVA upon the gel-forming processes in LDPE-EVA films. Radiat Phys Chem 1998;51(2):205–6.
[45] Sharif J, Aziz SHSA, Hashim K. Radiation effects on LDPE/EVA blends. Radiat Phys Chem 2000;58:191–5.
[46] Charlesby A. Atomic radiation and polymers. Oxford: Pergamon Press; 1960.
[47] Socrates G. Infrared characteristic group frequencies. New York, NY: Wiley Interscience; 1980.
[48] Allen NS, Edge M, Rodriguez M, Liauw CM, Fontan E. Aspects of the thermal oxidation, yellowing and stabilisation of ethylene vinyl acetate copolymer. Polym Deg Stab 2001;71:1–14.
[49] Crank J. The mathematics of diffusion. 2nd ed. Oxford: Clarendon Press; 1975.
[50] Vieth WR. Diffusion in and through polymers. Munich: Hansen; 1991.
[51] Anderson M, Shive MS. Biodegradation and biocompatibility of PLA and PLGA microspheres. Adv Drug Deliv Rev 1997;28:5–24.
[52] Spilizewski KL, Marchant RE, Hamlin CR, Anderson JM, Tice TR, Dappert TO, et al. The effect of hydrocortisone acetate loaded poly(DL-lactide) films on the inflammatory response. J Control Release 1985;2:197–203.